CHIN. PHYS. LETT. Vol. 36, No. 11 (2019) 114202

High-Repetition-Rate and High-Beam-Quality Laser Pulses with 1.5 MW Peak Power Generation from a Two-Stage Nd:YVO_4 Amplifier *

Qiu-Run He(何秋润)[1], Jing Guo(郭靖)[2], Bao-Fu Zhang(张宝夫)[1**], Zhong-Xing Jiao(焦中兴)[1,3**]

[1]*School of Physics, Sun Yat-sen University, Guangzhou 510275*

[2]*Sino-French Institute of Nuclear Engineering and Technology, Sun Yat-sen University, Zhuhai 519082*

[3]*National Demonstration Center for Experimental Physics Education, Sun Yat-sen University, Guangzhou 510275*

(Received 13 August 2019)

We develop a two-stage end-pumped Nd:YVO_4 amplifier seeded by a passively Q-switched microchip laser. An average output power of 13.5 W with repetition rate up to 7 kHz and pulse duration of ∼1.24 ns is obtained, corresponding to a pump extraction efficiency of 16.1% (19.5% for the second stage) and peak power of ∼1.5 MW. The beam quality factors at maximum output power are measured to be $M_x^2 = 1.56$ and $M_y^2 = 1.48$. We introduce an analytical model to estimate gain and beam quality after amplification. This model focuses on the influence of ratio of seed spot radius to pump spot radius when designing an amplifier. Moreover, our experiments reveal that the re-imaging system in the double-pass configuration can be used to enhance the beam quality.

PACS: 42.55.−f, 42.55.Xi, 42.60.Lh DOI: 10.1088/0256-307X/36/11/114202

Picosecond or nanosecond 1-μm lasers with high average power and good beam quality are attractive for many scientific and industrial applications. Master oscillator power amplifier (MOPA) architectures are found to be important candidates to achieve laser pulses with these two properties because of their flexibility and compactness. Many works about Nd:YVO_4 or Nd:YAG based MOPA laser systems have been reported in the past few years.[1−10] At the repetition rate of < 100 Hz, the laser pulse energy can reach hundreds of mJ.[1,2] Such high pulse energy is desirable for industrial material processing but low repetition rate is a limitation for processing speed. Therefore, it is necessary to make a balance between these two parameters in the MOPA laser systems. For this purpose, a Nd:YAG single-crystal fiber laser amplifier which delivered 2.7-mJ 450-ps pulses at 1 kHz was developed, corresponding to extraction efficiency of 33.9%,[7] a three-stage 5-kHz picosecond Nd:YAG slab amplifier producing multi-mJ pulses (extraction efficiency ∼ 4.4%) and its improved work (extraction efficiency ∼ 6.7%) have been reported,[8,9] a high-energy burst-mode Nd:YVO4/Nd:YAG MOPA laser generating 73-mJ 9.3-ns pulses at 10 kHz (extraction efficiency ∼14.4%) was demonstrated.[10] Those multi-kHz laser systems, which delivered multi-mJ pulses, show great potential in material processing but the high cost of the crystal fiber, their complex design and low pump extraction efficiency can be barriers for their practical application.

In this Letter, we present a high-efficiency MOPA laser system at multi-kHz. Seeded by a microchip laser with its average power of 310 mW, the amplifier contained a single-pass stage and a double-pass stage. The laser system generates pulses with the duration of 1.24 ns at 7 kHz. The maximum pulse energy of 1.93 mJ has been achieved, with the beam quality factors of $M_x^2 = 1.56$ and $M_y^2 = 1.48$. Total extraction efficiency of the amplifier is 16.1% (9.1% for the first stage and 19.5% for the second stage). Considering the gain guiding effect, temperature dependency of stimulated emission cross section, the energy transfer upconversion effect (ETU) and the recovery time between pulses, a theoretical model was built to analyze the gain and beam quality after laser amplification. The model predicted the influence of ratio of seed spot radius to pump spot radius (ω_l/ω_p) on gain and beam quality in theory. In addition, we found that the re-imaging system in the double-pass stage could be used for beam quality enhancement.

A schematic diagram of the first-stage amplifier is shown in Fig. 1. A passively Q-switched microchip laser at 1064 nm was chosen as the seed source for its compactness and reliability. The microchip laser operated at 7 kHz with pulse duration of ∼930 ps and average power of 310 mW. Its beam quality factors were measured to be $M_x^2 = 1.11$, $M_y^2 = 1.09$ by a beam quality analyzer (Spiricon M^2-200). An isolator was used to prevent feedback, which might lead to perturbation or even optical damage to the seed laser. A half wave plate (HWP1) was employed to adjust the polarization of the beam to optimize the amplification efficiency. A plano-convex lens (L1) focused the seed laser beam into an a-cut 0.3 at.% doped Nd:YVO_4 composite crystal. The crystal has a size of 3 mm ×3 mm × (2+16+2) mm where 2 mm refers the length of undoped YVO_4 crystal in both ends, and it was trapped in indium foil and mounted in a water-cooled copper holder. The radius of the signal beam spot inside the crystal was 200 μm. The pump laser

*Supported by the Natural Science Foundation of Guangdong Province under Grant Nos 2017A030310305 and 2018A030310092, and the Young Teachers Training Program of the Fundamental Research Funds for Sun Yat-sen University under Grant No 20174500031610017.

**Corresponding author. Email: zhangbf5@mail.sysu.edu.cn; jiaozhx@mail.sysu.edu.cn

© 2019 Chinese Physical Society and IOP Publishing Ltd

(878 nm, 30 W) was coupled into the crystal by an aspheric doublet (Coupler1). The pump spot radius was 250 μm inside the crystal. The pump absorption efficiency of the crystal was measured to be 88%.

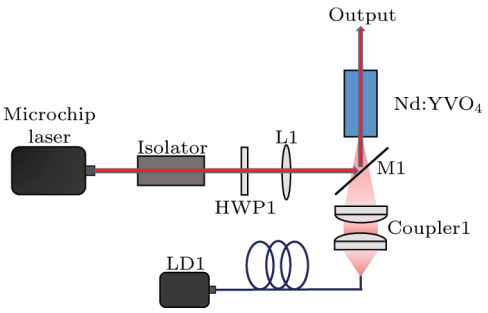

Fig. 1. Schematic setup of first-stage single-pass amplifier.

The schematic setup of second-stage amplifier is depicted in Fig. 2. A polarizing beam splitter (PBS) and a 45° Faraday rotator (FR) were employed as an optical isolator and the output port of the amplified laser. The polarization of the beam was adjusted by HWP2, and thus the beam could pass through PBS completely. Here, the function of HWP3 was the same as HWP1. The input laser beam was expanded by a combination of a concave lens (L2) and a convex lens (L3), resulting in a spot radius of 300 μm inside the Nd:YVO_4 crystal. This crystal had the same parameters and condition as the one used in the first-stage amplifier. It was end-pumped by an 808-nm 100-W laser diode (LD2) through a coupling system (Coupler2). The pump spot radius was 375 μm in this stage. The pump absorption efficiency of the crystal was measured to be 90%. A re-imaging system consisting of a convex lens (L4, $f = 75$ mm) and a plane mirror (M5) was used, and the distances $D1$ and $D2$ were experimentally optimized as 122 mm and 46 mm. The effect of re-imaging system will be discussed in the following.

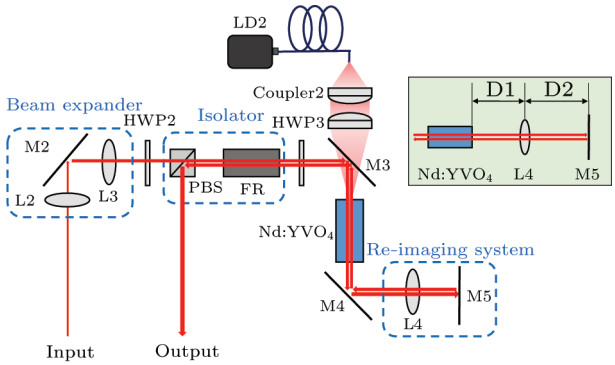

Fig. 2. Schematic setup of second-stage double-pass amplifier. Inset: diagram of the re-imaging system.

The performance of the laser system was achieved using a power meter (Newport, 1916-R), a 2-GHz digital phosphor oscilloscope (Tektronix, DPO5204B) coupled with an InGaAs photodetector (Thorlabs, DET025 A), and a beam quality analyzer (Spiricon M^2-200).

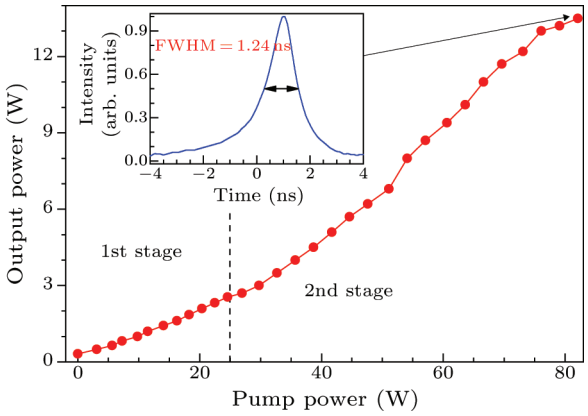

Fig. 3. Output power versus pump power for the two-stage amplifier. Inset: laser pulse trace at the maximum output power.

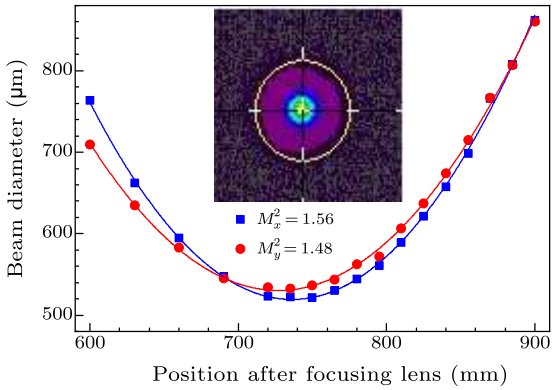

Fig. 4. The M^2 measurements of the laser at the maximum output power. Inset: beam intensity distribution at near field.

As shown in Fig. 3, the average power rose to 2.55 W after the first-stage amplification. The gain of the first-stage amplifier was 8.2 and the corresponding extraction efficiency was 9.1%. The beam quality factors were measured to be $M_x^2 = 1.13$ and $M_y^2 = 1.11$. The first-stage amplifier was supposed to be high-gain and meanwhile high-beam-quality. The experimental results met this expectation, attributing to good matching between the input signal spot and the pump spot. Passing through HWP2, Isolator and HWP3, the signal beam suffered from power loss and the average power decreased to 2.3 W. After the second-stage amplification, the average power was amplified to 13.5 W in the pump power of 57.5 W. The gain of the second-stage amplifier was 5.9 and the corresponding extraction efficiency was 19.5%. The pulse duration here was broadened to ~1.24 ns. The corresponding beam quality factors were measured to be $M_x^2 = 1.56$ and $M_y^2 = 1.48$ (presented in Fig. 4). In summary, the amplifier provided the output beam with high power and good quality.

In the following, we investigate the influence of laser beam radius ω_l and pump beam radius ω_p on the gain and beam quality of an amplifier. As to pulse

amplification, the output fluence after a single-pass amplifier is given by[11,12]

$$E_{\rm out}(r) = E_{\rm s} \ln\left\{1 + \left[\exp\left(\frac{E_{\rm in}(r)}{E_{\rm s}}\right) - 1\right] G_{\rm i}\right\}, \quad (1)$$

where $E_{\rm in}(r)$ is the input signal fluence, $E_{\rm s} = \frac{h\nu_{\rm l}}{\sigma_{21}}$ is the saturation fluence, and $G_{\rm i}$ is the initial gain at the time of arrival of a pulse. For a signal beam with good quality, the signal beam intensity profile can be simply approximated as a Gaussian profile, and it can be written as

$$E_{\rm in}(r) = \frac{I_{\rm in}(r)}{f} = \frac{2P_{\rm i}}{\pi f \omega_{\rm l}^2} \exp\left(\frac{-2r^2}{\omega_{\rm l}^2}\right), \quad (2)$$

where $P_{\rm i}$ is the input power, f is the repetition rate, and $\omega_{\rm l}$ is the $1/e^2$ width of input signal beam. Usually, the gain $G_{\rm i}$ in Eq. (1) can be approximated to $G_{\rm i} = \exp(g_0 l) = \exp(n\sigma_{21} l)$. Taking Auger upconversion effects into account, the population density could be calculated by[13]

$$n(r) = \left[\sqrt{1 + 4\tau_{\rm f}^2 \gamma R(r)} - 1\right] / 2\tau_{\rm f}\gamma, \quad (3)$$

where $\tau_{\rm f}$ is the upper level lifetime, $\gamma = 3.6 \times 10^{-15}/{\rm cm}^3/{\rm s}/{\rm at.}\%$ is the upconversion coefficient,[14] and $R(r) = \frac{I_{\rm p}(r)\eta_{\rm abs}}{h\nu_{\rm p} l}$ ($\eta_{\rm abs}$ is total fraction of pump power absorbed over the length of gain medium l) is the rate of the pump intensity. In this experiment, $I_{\rm p}(r)$ has a truncated Gaussian profile, and it can be written as

$$I_{\rm p}(r) = \begin{cases} \frac{1.69P_{\rm p}}{\pi\omega_{\rm p}^2} \exp\left(\frac{-1.16r^2}{\omega_{\rm p}^2}\right), & r \leqslant \omega_{\rm p}, \\ 0, & r > \omega_{\rm p}, \end{cases} \quad (4)$$

where $P_{\rm p}$ is the pump power, and $\omega_{\rm p}$ is the $1/e^2$ width of pump beam.

When $1/f$ is comparable to $\tau_{\rm f}$, the recovery time between pulses should be taken into account in the approximation of $G_{\rm i}$. The gain with respect to the recovery time $t_{\rm r} = 1/f - t_{\rm p}$ ($t_{\rm p}$ is the pulse duration) between pulses is given by[15]

$$G(t_{\rm r}) = \exp\left\{g_0 l\left[1 - \exp\left(\frac{-t_{\rm r}}{\tau_{\rm f}}\right)\right] + \ln G_{\rm e} \exp\left(\frac{-t_{\rm r}}{\tau_{\rm f}}\right)\right\}, \quad (5)$$

where $G_{\rm e} = 1 + (G_{\rm i} - 1)\exp(\frac{E_{\rm out}}{E_{\rm in}})$ is the gain during the pulse. Note that we here use the steady value of $G_{\rm i}$ to model the gain of the amplifier. The steady value can be obtained by applying Eqs. (1) and (5) iteratively and each time replacing the initial gain in Eq. (2) with new gain in Eq. (5).

Innocenzi *et al.* provided an analytic approximation about the radial temperature distribution in the crystal.[16] To simplify calculation, we fit the temperature distribution with the function $T(r) = A\exp(-Br^2)$, where A and B are the fitting parameters. The temperature dependency of stimulated emission cross section for Nd:YVO_4 can be estimated by[17]

$$\sigma_{21}(T) = 2.2 \times 10^{-18}({\rm cm}^2) - 4 \times 10^{-21}({\rm cm}^2/^\circ{\rm K}) * T(^\circ{\rm K}). \quad (6)$$

Finally, the energy gain of the amplifier can be calculated by

$$G = \frac{\int E_{\rm out}(r) 2\pi r dr}{\int E_{\rm in}(r) 2\pi r dr}. \quad (7)$$

Siegman's model describes the relationship between the final beam quality $M_{\rm f}^2$ after passing through the gain medium and the initial beam quality $M_{\rm i}^2$ of input signal beam.[18,19] To improve his model, gain guiding effect should be taken into account because of its remarkable influence on output beam profile and beam quality.[2,20,21] To simplify the theoretical model instead of solving it with numerical method,[20] we here assume that the gain guiding effect does not change the far-field divergence angle of the beam but only changes the beam radius at the gain medium. To quantify this change, the factor $q = \omega_{\rm l}'/\omega_{\rm l}$ is defined as a ratio of output beam width to signal beam width. The output beam width $\omega_{\rm l}'$ can be calculated by the second moment of the beam intensity profile[22]

$$\omega_{\rm l}' = \sqrt{\frac{4\int \pi r^3 E_{\rm out}(r) dr}{\int 2\pi r E_{\rm out}(r) dr}}. \quad (8)$$

We take the gain guiding effect factor q into Siegman's model, and the final beam quality can be evaluated as

$$M_{\rm f}^2 = \sqrt{(M_{\rm i}^2)^2 + (M_{\rm q}^2)^2} * q, \quad (9)$$

where $M_{\rm q}^2$ is the beam quality degradation factor for a quartic phase aberration.[19]

In addition, the thermal lens focal length at $r = 0$ in the crystal could be calculated by[12]

$$f_{\rm th} = \frac{2\pi K_{\rm c} \omega_{\rm p}^2}{1.69 P_{\rm p} \gamma \eta_{\rm abs} (dn/dt)}. \quad (10)$$

To verify the accuracy of the model, we first built up a typical single-pass end-pumped amplifier, whose configuration is shown in Fig. 5. A 7-kHz laser beam with its average power of 7.7 W and beam quality factor of $M^2 = 1.31$ was focused into an a-cut 0.3 at.% doped Nd:YVO_4 composite crystal. The crystal had a size of 3 mm ×3 mm × (2+16+2) mm, and it was end-pumped by an 808-nm laser diode (LD). The signal beam radius inside the crystal was 260 μm. The function of HWP was the same as HWP1 in Fig. 1. The absorption efficiency of the crystal was 90%. The power and beam quality of output beam were measured when changing the pump beam radius from 260 μm to 570 μm.

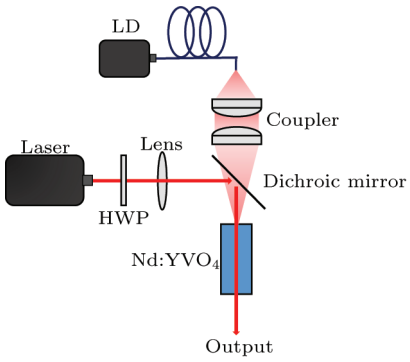

Fig. 5. Experimental setup of a typical single-pass end-pumped amplifier.

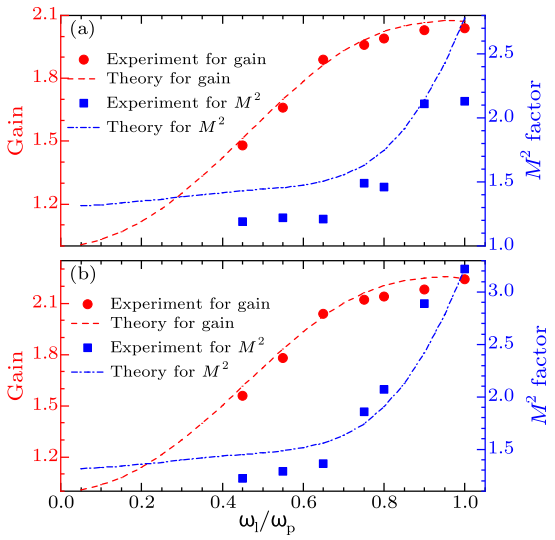

Fig. 6. Gain and M^2 factor versus ω_l/ω_p value when the pump power is (a) 32.5 W and (b) 39 W.

As shown in Fig. 6, the experimental and the theoretical results follow a relatively consistent trend: the power gain in the amplifier keeps in growing with increasing ω_l/ω_p, the output beam quality becomes worse as ω_l/ω_p grows, especially when ω_l/ω_p is over 0.8. As to the power gain, there is good agreement between the models and the experimental results, which indicates the accuracy of the model. Different parameter values from different references also affect the model results, but the effect can be limited in a reasonable range. Moreover, neglect of gain distribution in the direction of beam propagation can also lead to a decline in accuracy of the gain model, especially when a low-doping and long crystal is employed. As to the beam quality, the theoretical values are not consistent with the experimental results accurately. In the high power regime, complex thermal effects make it difficult to calculate the beam quality. The differences between the experimental and the theoretical results are caused by the limitation of the degradation factor for a quartic phase aberration, complexity of the actual beam profile, and the simple assumption of unchanged far-field divergence angle in this model. In addition, the simulation about beam quality would be unreliable in the case of ω_l/ω_p over 1. In this case, the quartic phase aberration approximation is invalid and other effects play more important roles. In summary, this model may not predict accurate results of the power gain and the beam quality but it does give an appropriate guidance for the design of amplifier when considering the influence of ω_l and ω_p.

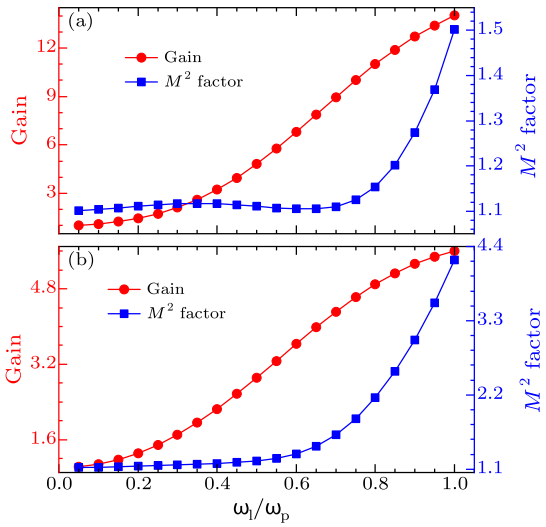

Fig. 7. Theoretical power gain and M^2 factor versus ω_l/ω_p value in (a) the first-stage amplifier when the pump power is 24.5 W, and (b) the first pass of the second-stage amplifier when the pump power is 57.5 W.

With this model mentioned, we calculate the gain and the beam quality for the first stage and the first pass of the second stage. The simulation results are presented in Fig. 7. As for the first stage, to obtain high gain and meanwhile keep a good quality, it can be seen that the optimal range of ω_l/ω_p value is 0.75–0.85. In this range, the expected gain is high (over 9) and the expected beam quality is good (M^2 less than 1.4). In the first stage, the experimental ω_l/ω_p value ~0.8 and amplification results (power gain ~8.2, beam quality $M_x^2 = 1.13$ and $M_y^2 = 1.11$), support the analysis about the optimal range of ω_l/ω_p value.

As for the second stage, the simulation results show that, when ω_l/ω_p is over 0.8, the beam quality deteriorates rapidly as ω_l/ω_p increases, and the slope efficiency of the gain begins to drop significantly. Therefore, the experimental value was also set to be ~0.8 in the second stage. In this case, the calculated gain in the first pass is 4.90 and the corresponding beam quality M^2 is 2.16. As to the second pass, according to conventional amplification theory, the beam quality will be deteriorated again for thermal spherical aberration, thus the theoretical beam quality after double-pass amplification will be worse than the quality after the first pass. However, our experimental results showed that the power gain in the second stage was ~5.9 and the beam quality was measured to be $M_x^2 = 1.56$ and $M_y^2 = 1.48$. The experimental gain is higher than the simulation results because only the gain for the first pass is calculated and the second

pass provides additional gain. As to beam quality, it is fairly interesting that the experimental beam quality is better than the simulation result. The improvement of the beam quality may attribute to the gain guiding effect.[20,21] The physical mechanism of the gain guiding effect is suppressing the gain of higher modes in the signal beam and meanwhile enhancing the gain of fundamental mode. According to Ref. [21], under the conditions of ω_l slightly larger than ω_p and input beam with bad beam quality, the gain guiding effect will be strengthen significantly and the thermal effect will be weakened, leading to a beam quality improvement. To confirm the strengthening of the gain guiding effect and compare the re-imaging system with other double-pass configuration, we estimate the second-pass beam radius inside the crystal versus pump power in the re-imaging system and the 'Reflector Only' configuration. ABCD matrix is used to complete the calculation, considering the changes of beam quality after the first pass and the thermal lens. The results are shown in Fig. 8. We can see that in the second pass with a re-imaging system, the theoretical ω_l is ~369 μm when the pump power is 57.5 W. Under the conditions of poor quality of the input beam ($M^2 = 2.16$) and ω_l close to ω_p (375 μm), the gain guiding effect was strengthened, and thus improved the beam quality in the second pass. An optimized Reflector Only configuration may have a similar effect in such situation. However, when the amplifier is pumped with lower power, the Reflector Only configuration has a smaller second-pass beam radius and thus lower gain.

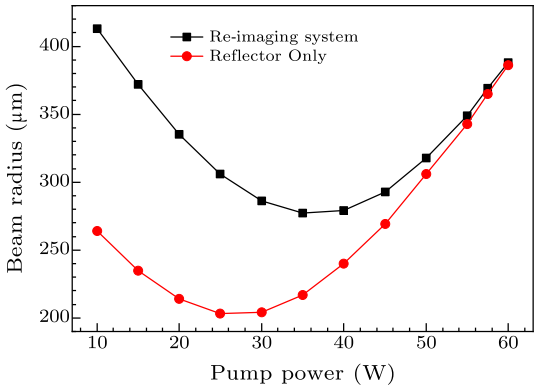

Fig. 8. The second-pass beam radius inside the crystal versus pump power in the re-imaging system and the Reflector Only configuration.

In conclusion, we have built a two-stage Nd:YVO_4 MOPA laser system. The maximum average power of 13.5 W and corresponding pulse energy of 1.93 mJ are achieved after two-stage amplification. The total gain of the two-stage amplifier reaches 43.5 (8.2 for the first stage and 5.9 for the second stage), and the corresponding extraction efficiency is 16.1% (9.1% for the first stage and 19.5% for the second stage). The beam quality factors of the maximum output power are measured to be $M_x^2 = 1.56$ and $M_y^2 = 1.48$. The theoretical model considering gain guiding effect, temperature dependency of stimulated emission cross section, ETU and the recovery time between pulses, predicts the influence of value on gain and beam quality in theory. In the experiment, we find that the re-imaging system in double-pass configuration can improve the beam quality because of gain guiding effect. Our work provides a simple and compact design of nanosecond or sub-nanosecond MOPA system with high pulse energy and high power at multi-kHz, which shows great potential in industrial material processing.

References

[1] Maleki A, Kavosh Tehrani M, Saghafifar H, Moghtader Dindarlu M H and Ebadian H 2016 *Laser Phys.* **26** 025003
[2] Yahia V and Taira T 2018 *Opt. Express* **26** 8609
[3] Liu B and Liu C 2016 *Lasers Congress 2016 (ASSL, LSC, LAC)* (Boston, USA 30 October–3 November 2016) p JTu2A.21
[4] Agnesi A, Carrà L, Pirzio F and Reali G 2012 *Appl. Phys. B* **109** 659
[5] Agnesi A, Carrà L, Piccoli R, Pirzio F and Reali G 2012 *Opt. Lett.* **37** 3612
[6] Yoshino T, Seki H, Tokizane Y, Miyamoto K and Omatsu T 2013 *J. Opt. Soc. Am. B* **30** 894
[7] Martial I, Balembois F, Didierjean J and Georges P 2011 *Opt. Express* **19** 11667
[8] Chen Y, Li F Q, Liu K, Xu H Y, Zong N, Guo Y D, Zhang S J, Zhang J Y, Peng Q J, Bo Y, Cui D F and Xu Z Y 2015 *IEEE Photon. Technol. Lett.* **27** 1531
[9] Chen Y, Liu K, Yang J, Yang F, Gao H, Zong N, Yuan L, Lin Y, Liu Z, Peng Q, Bo Y, Cui D and Xu Z 2016 *J. Opt.* **18** 075503
[10] Li X, Yan R, Zhou Y, Ma Y, Chen D and Zhou Z 2017 *Conf. Lasers Electro-Opt.* (San Jose USA 14–19 May 2017) p JW2A.93
[11] Koechner W 2006 *Solid-State Laser Engineering* (New York: Springer)
[12] Yarrow M J 2006 *PhD Dissertation* (Southampton: University of Southampton)
[13] Chen Y F, Liao C C, Lan Y P and Wang S C 2000 *Appl. Phys. B* **70** 487
[14] Délen X, Balembois F and Georges P 2012 *J. Opt. Soc. Am. B* **29** 2339
[15] Yarrow M J, Kim J W and Clarkson W A 2007 *Opt. Commun.* **270** 361
[16] Innocenzi M E, Yura H T, Fincher C L and Fields R A 1990 *Appl. Phys. Lett.* **56** 1831
[17] Turri G, Jenssen H P, Cornacchia F, Tonelli M and Bass M 2009 *J. Opt. Soc. Am. B* **26** 2084
[18] Siegman A E 1993 *Appl. Opt.* **32** 5893
[19] Clarkson W A 2001 *J. Phys. D* **34** 2381
[20] Yan X, Liu Q, Fu X, Wang D and Gong M 2010 *J. Opt. Soc. Am. B* **27** 1286
[21] Xiang Z, Wang D, Pan S, Dong Y, Zhao Z, Li T, Ge J, Liu C and Chen J 2011 *Opt. Express* **19** 21060
[22] Siegman A E 1998 *Diode Pumped Solid State Lasers: Applications and Issues* (Washington D.C. USA 1 January 1998) p MQ1